The Advection of Mesoscale Atmospheric Vortices over Reykjavík

HÁLFDÁN ÁGÚSTSSON

Belgingur-Institute for Meteorological Research, Icelandic Meteorological Office, and University of Iceland, Reykjavík, Iceland

HARALDUR ÓLAFSSON

University of Iceland, and Icelandic Meteorological Office, Reykjavík, Iceland, and Bergen School of Meteorology, Geophysical Institute, University of Bergen, Bergen, Norway

(Manuscript received 14 February 2013, in final form 12 February 2014)

ABSTRACT

On 12 August 2009, a series of satellite images revealed asymmetric shedding of atmospheric vortices in the lee of Mt. Snæfellsjökull, and their passage a distance of 120 km across Faxaflói Bay and over the city of Reykjavík in West Iceland. After landfall, the vortices were detected by a network of surface weather stations. These observations are presented and with the aid of a numerical simulation, they are discussed in view of existing theories of orographic wakes and vortex shedding. In general, the flow is in line with existing knowledge, but there is a remarkable absence of vortices with anticyclonic rotation. Atmospheric conditions for vortices of this kind are most often favorable in late winter and spring and they are a forecasting challenge.

1. Introduction

Downstream of mountains, there is frequently an extended area of weak winds, referred to as a wake. Mountain wakes are of particular interest in studies of weather and climate because they feature a flow pattern and flow speed that may be very different from the ambient flow, which is most often reasonably well reproduced by numerical models, while the wake flow may not be well reproduced.

In general, mountain wakes are associated with background flow (upstream of the mountains) of strong static stability, weak winds, high mountains or all of the above. At values well above 1 of Nh/U, where N is the Brunt–Väisälä frequency, h is the mountain height, and U is the wind speed, the atmospheric flow is blocked on the upstream side of a mountain. Downstream, there is most often a wake that may extend large distances away from the mountain.

It is well established that vorticity may be produced in stratified flow that impinges on an obstacle (e.g., Smolarkiewicz and Rotunno 1989a,b; Smith 1989b; Hunt et al. 1997) and that potential vorticity and a reduction in the value of the Bernoulli function inside the wake is preceded by mixing and dissipation that may be distributed widely inside the wake region or be concentrated in regions of gravity wave breaking (Schär and Smith 1993a; Schär and Durran 1997).

Based on the work of Schär and Smith (1993a,b) and Grubišić et al. (1995), Smith et al. (1997) present wake flow regimes as a function of mountain height, critical mountain height for internal wave breaking, and the Reynolds number. When the mountain height is well above a critical mountain height for wave breaking and the surface Reynolds number is large, there is vortex shedding inside the wake. Earlier, a critical value of 0.4 of the Froude number had been established as an upper limit of the regime of vortex shedding (see Etling 1989, 1990). An extensive description of vortices in the atmospheric boundary layer downstream of a smooth mountain, based on numerical simulations with ultrahigh resolution and including series of sensitivity tests is given in Heinze et al. (2012).

On 12 August 2009, unique observations were made of vortex shedding downstream of Mt. Snæfellsjökull in West Iceland and the advection of the vortices over a dense network of automatic weather stations. This case is presented and discussed in the present paper.

Corresponding author address: Hálfdán Ágústsson, Institute for Meteorological Research, Orkugarði, Grensásvegi 9, 108 Reykjavík, Iceland.
E-mail: halfdana@gmail.com

DOI: 10.1175/MWR-D-13-00060.1

© 2014 American Meteorological Society

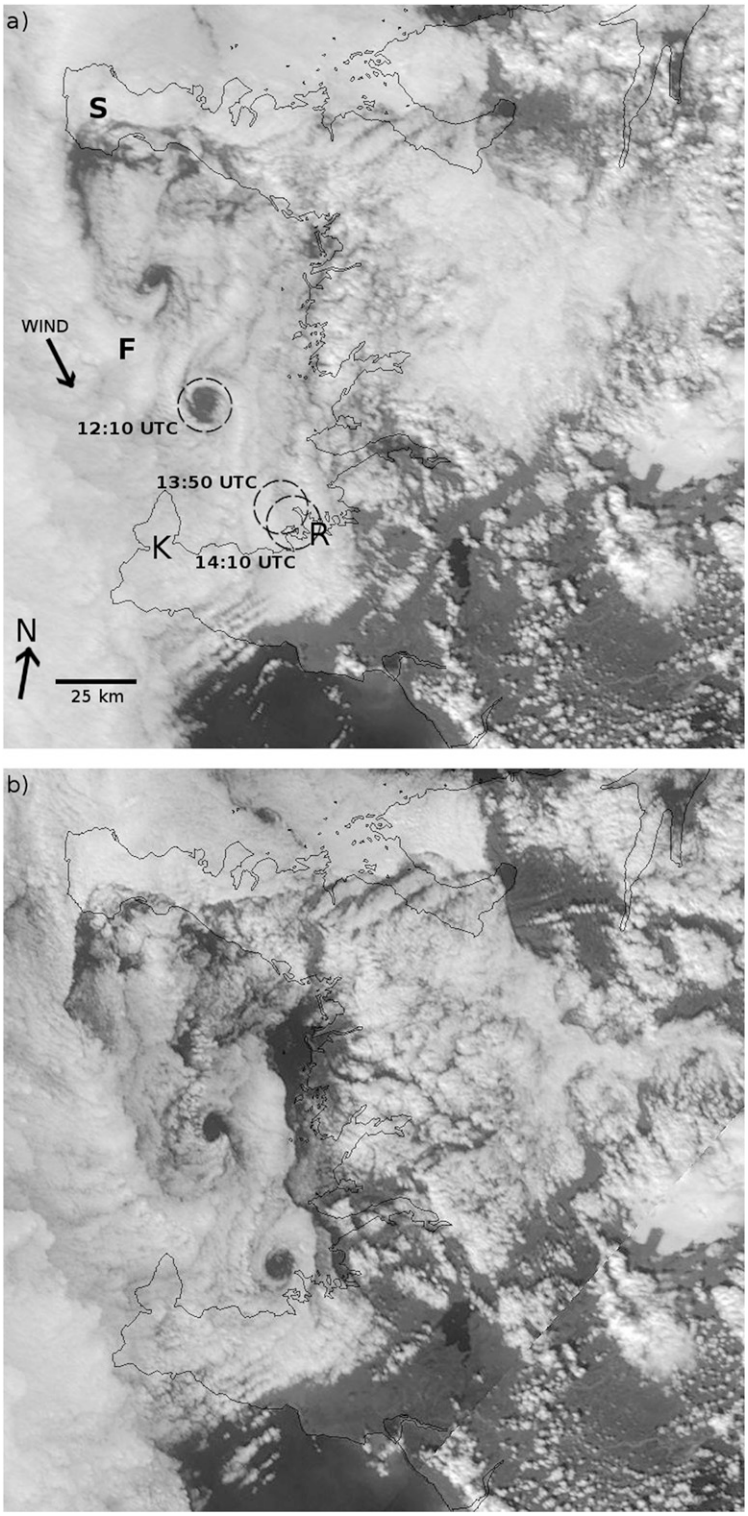

FIG. 1. Moderate Resolution Imaging Spectroradiometer (MODIS) images (visible light, 250-m resolution) from the *Terra* and *Aqua* satellites showing a part of West Iceland at (a) 1210, (b) 1350, and (c) 1410 UTC 12 Aug 2009. Also shown in (a) are the coastline, the locations of Mt. Snæfellsjökull (S), Reykjavík (R), Keflavík (K), the Faxaflói bay (F), the direction of the large-scale flow, as well as the location of the first vortex in the three satellite images.

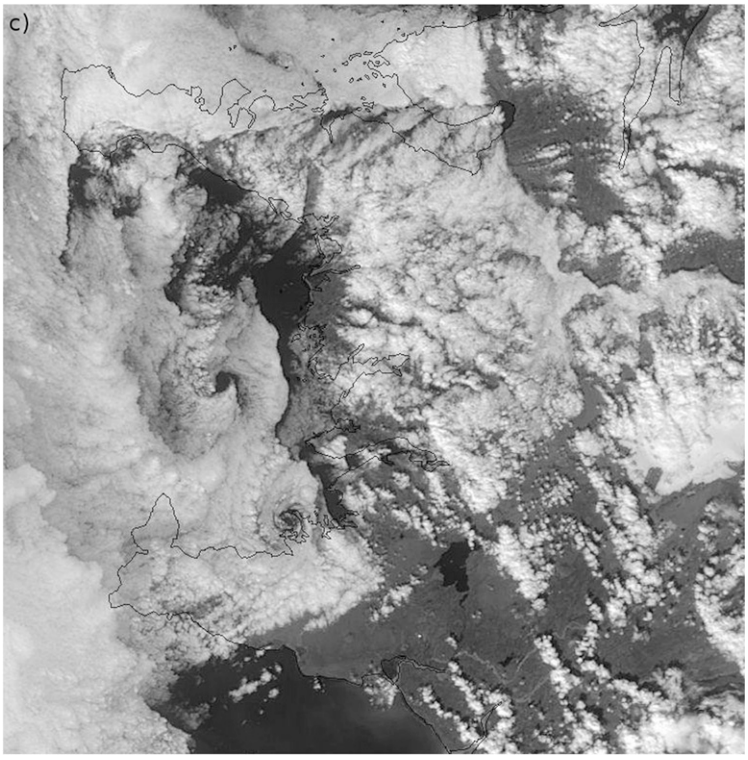

FIG. 1. (*Continued*)

2. The atmospheric flow, generation, and shedding of the vortices

On 12 August 2009, a series of consecutive satellite images (Fig. 1) documented the advection of two atmospheric vortices across the Faxaflói Bay in West Iceland and their passage above the city of Reykjavík, Iceland. A third vortex can also be detected, but not as clearly as the first two. A pattern of elongated clouds wrapped up in a circle with a localized clearing in a layer of stratus or stratocumulus clouds is associated with the vortices and makes them visible in the satellite imagery. Both the observed vortices rotate counterclockwise and were shed from Mt. Snæfellsjökull, a glacier-capped mountain reaching 1446 m above mean sea level (MSL). Mt. Snæfellsjökull is located at the westernmost tip of the approximately 80-km-long Snæfellsnes peninsula, which has an average height of a few hundred meters with some 15 individual peaks rising to 800–1000 m MSL.

Upper-air observations from Keflavík, Iceland, at 1200 UTC 12 August 2009 (Fig. 2), 100 km to the south of Mt. Snæfellsjökull (but outside its wake), show a 3–4-K inversion at 900 hPa (1000 m) with winds of 5–6 m s^{-1} from the northwest in the atmospheric boundary layer. The sounding reveals a thin layer of clouds at the top of the boundary layer, above which the air is dry. Earlier that day, the inversion was very close to the surface and in the evening the same day, the winds in the boundary layer turned to the west and later southwest.

According to the satellite images, the vortices were advected some 120 km to the southeast, across Faxaflói Bay in the same direction as the ambient flow at a speed of 5–6 m s^{-1}, which is similar to the boundary layer wind speed in the sounding at Keflavík at 1200 UTC. The satellite images indicate that the shedding period at the mountain is close to 2 h.

The mean sea level pressure is shown in Fig. 3. There is a ridge of high pressure to the west of Iceland, leading to a northwesterly breeze over West Iceland. No high-resolution satellite images are available in the late afternoon, but veering of the winds toward a more westerly direction (putting the Snæfellsnes mountain range in the place of the Snæfellsjökull wake) suggests that there were no more vortices that day.

Approximately 5 h after the creation of the first vortex, it passed above the city of Reykjavík. Its passage over the city and further inland is documented by a dense network of automatic weather stations in the Reykjavík region (Figs. 4 and 5). Changes in the wind speed and wind direction at 10 m above ground level are an indicator of the passage of the vortex aloft. At Veðurstofa Íslands (VI; the Icelandic Meteorological Office) observations

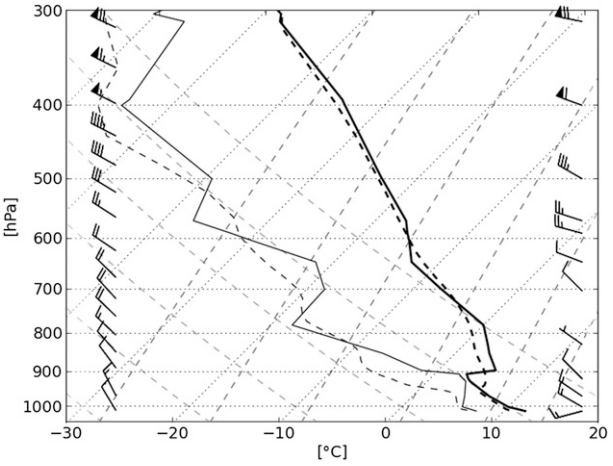

FIG. 2. Skew T–log$p$ diagram from the Keflavík upper-air station in southwest Iceland (Fig. 1) at 1200 UTC 12 Aug 2009. Shown are observed (solid lines) and simulated at 1-km resolution (dashed lines) temperature (dark gray, °C) and dewpoint (light gray, °C) as well as wind barbs (2.5 m s^{-1} each half barb, observed to the right and simulated to the left) with temperature/dewpoint on the lower axis and height (hPa) on the vertical.

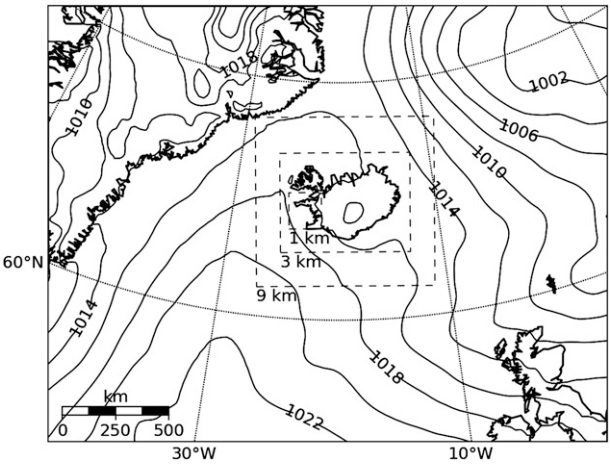

FIG. 3. Mean sea level pressure (hPa) in the ECMWF analysis at 1200 UTC 12 Aug 2009. Also shown are the locations of the numerical domains, with the extent of the innermost domain similar to that of the satellite images in Fig. 1.

of solar radiation show a continuous clearing in the cloud cover from 1410 to 1440 UTC, corresponding nicely to the size and the speed of the eye of the first vortex in Fig. 1c.

After landfall, this vortex travels with similar speed as before. It can be traced for more than 1 h (25 km) using gradually weakening signals in the observed winds from six automatic weather stations, starting at 1410 UTC at the westernmost weather station and ending at 1520 UTC at the easternmost station in Fig. 5. As it progressed farther inland it presumably either missed the subsequent weather stations or had weakened too much to be detected in the convective boundary layer over the land.

The vertical structure of the low-level atmosphere revealed by the Keflavík radiosounding at 1200 UTC 12 August 2009 (i.e., a shallow layer of cold northerly winds capped by potentially warmer air with weaker winds) is not uncommon. Such structures, but with much stronger winds are well known to be associated with violent downslope winds in the winter (Ólafsson and Ágústsson 2007; Ágústsson and Ólafsson 2012). Here, the low-level air mass arrives from the cold ocean at the east coast of Greenland, while the air mass above the inversion arrives from the west and is subjected to subsidence on the eastern side of a mid- to upper-level ridge (Fig. 6).

3. Numerical simulations

To establish a clearer picture of the vortices and the atmosphere in which they are embedded, the flow has been simulated with the nonhydrostatic mesoscale Advanced Research Weather Research and Forecasting (WRF) Model (ARW; Skamarock et al. 2005) with initial data from the European Centre for Medium-Range Weather Forecasts (ECMWF) operational analysis. The simulation domains are shown in Fig. 3. Their horizontal resolution is 9, 3, and 1 km and there are 55 vertical levels. The flow was also simulated with Interim ECMWF Re-Analysis (ECMWF-Interim) data and with Global Forecast System (GFS) data as well as with the upper-air observations from Keflavik Airport as constant initial and boundary conditions. None of these simulations gave better results in terms of creation and shedding of vortices, and shall not be discussed further. All the available PBL parameterization schemes were tested. Only results from the simulation producing the best results in terms of the depth of the boundary layer and the sharpness of the inversion are presented here. They are obtained using the Yonsei University (YSU) PBL scheme (Hong et al. 2006; see also Shin and Hong 2011) which is a first-order closure scheme. The scheme considers nonlocal mixing by convective large eddies. It expresses nonlocal mixing by adding a nonlocal gradient term to the local gradient of each prognostic mean variable for heat and momentum components.

A clear signal of shedding vortices or plumes of warm air are present in the simulation, but the vortices are somewhat more diffuse than those observed; that is, the simulation underestimates the turning of the surface winds and the structured and stable circular flow pattern observed in the satellite images is not quite as remarkable in the simulation. This could possibly be due to details in the vertical structure of the upstream flow, but is more likely due to too much mixing at the top of the boundary layer. A slight underestimation of the height

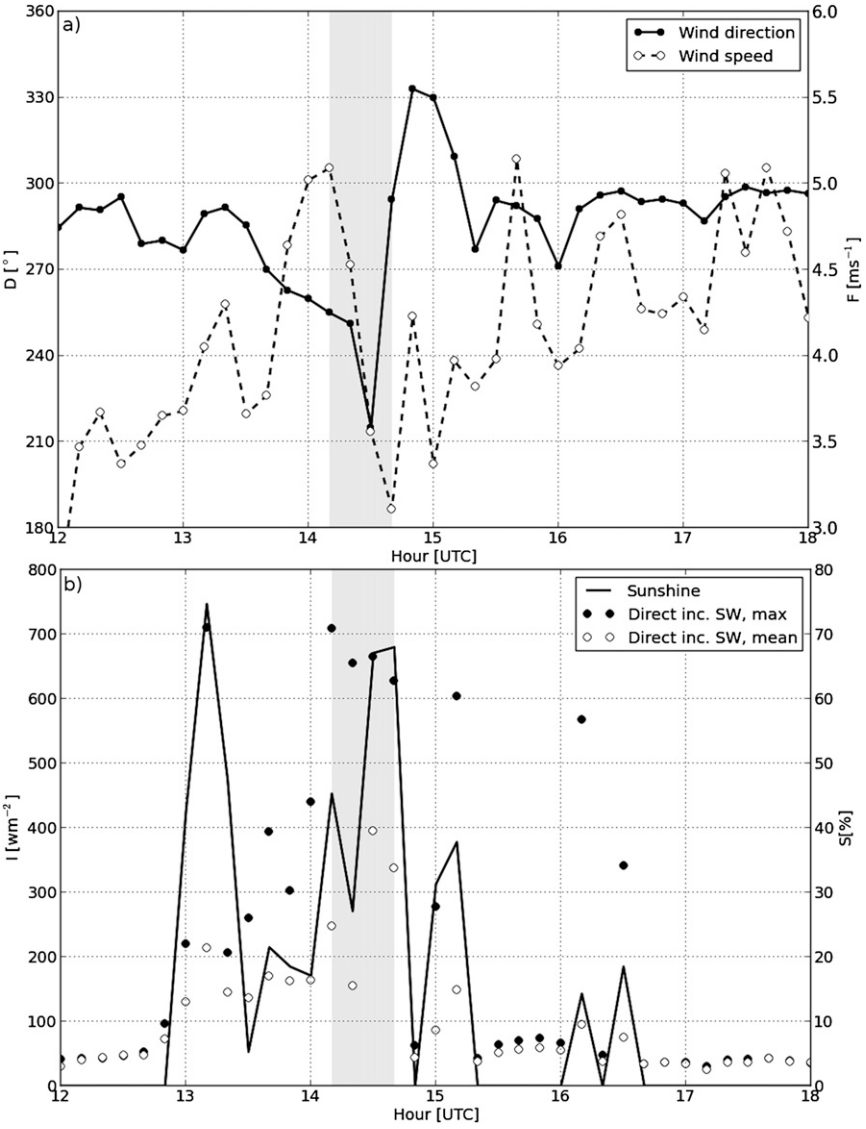

FIG. 4. Observations of (a) 10-m wind speed F and direction D and (b) incoming solar radiation I and sunshine S at VI (Fig. 5). The time of the vortex above the station is depicted by the shaded region.

of the mountain at 1-km resolution (about 100-m difference between the real plateau below the narrow peaks and the top of the model topography) may also have an impact. There is a clear signal of a vortex in the local small-scale trough in the surface pressure (marked as 1 in Fig. 7), approximately two-thirds of the distance from Mt. Snæfellsjökull to Reykjavík. The model results are mostly correct, but even very small errors in the speed (1 m s^{-1}) and direction (10°–20°) of the impinging flow inevitably lead to errors in the location and time of landfall of the vortices several hours later. One simulated disturbance makes landfall at approximately 1400 UTC to the west of Reykjavík (not shown), coinciding quite well with the timing of the observed vortex in Fig. 5, but with a shift of several kilometers to the west when compared to observations. The model produces at least three vortices or plumes, two of which can be identified with those seen in the satellite imagery (Fig. 1) although they are shed a little too fast in the model. A third vortex signal is produced earlier and makes landfall at 1200 UTC (marked as 0 in Fig. 7), but is neither confirmed by the available satellite images, nor by the surface-based observations in the Reykjavík region. The vortices appear as localized minima in the wind field and maxima in the vorticity field (Fig. 8). The vortices are associated with localized curved minima in the relative humidity field (Fig. 9),

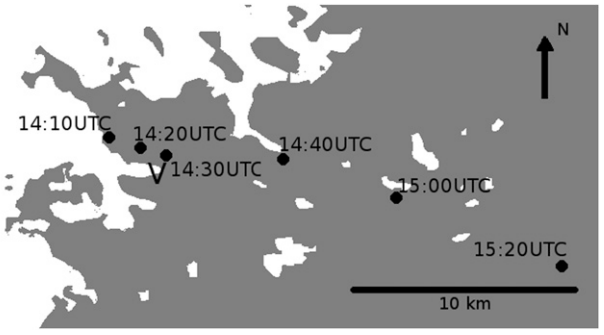

FIG. 5. Map of the Reykjavík region depicting the timing of the passage of the vortex aloft as deduced from changes in wind speed and direction at 10 m observed at automatic weather stations. The station at VI is marked with V (Fig. 4).

resembling the vortex pattern in Fig. 1. Aloft, the vortices are represented by columnar wind minima (Fig. 10) with small pockets of reversed flow at the top of the boundary layer. The vortices have a warm core and they are associated with a lowering of the top of the boundary layer.

To shed a light on the role of the orography on the Snæfellsnes peninsula, to the east of Mt. Snæfellsjökull, on the vortices and the flow in general, the atmosphere is simulated with these mountains removed. The results are shown in Figs. 8 and 10. In this simulation, there is an extended, narrow, and wavy wake, but no clear vortices. In the simulation where the mountains have been removed, there is stronger low-level flow over the east part of Faxaflói Bay, but the flow on each side of the wake of Mt. Snæfellsjökull, close to the mountain itself, is weaker than if the entire mountain range is present. Upstream, the stable layer is a little lower and more stable and the flow inside the boundary layer is a little faster if the mountain range is not present.

4. Seasonal variability

Winds from the northwest at mountain-top level and an inversion between approximately 925 and 850 hPa are obviously conditions that are favorable for wake creation with or without vortex shedding from Mt. Snæfellsjökull toward Reykjavík. An insight into the seasonal variability of such situations is given in Fig. 11. The columns indicate winds from the northwest at mountain-top level (850 hPa), coinciding with an inversion in the 925–850-hPa layer. There is high frequency in the late winter and the spring, but low frequency in the autumn and local minima in February and July. As the frequency of the weather conditions favorable for vortices of the kind described in the present paper is a combination of winds and static stability, both the frequency of northwesterly winds and the mean static stability are also presented in Fig. 11. The late winter/spring high frequency, the low autumn frequency,

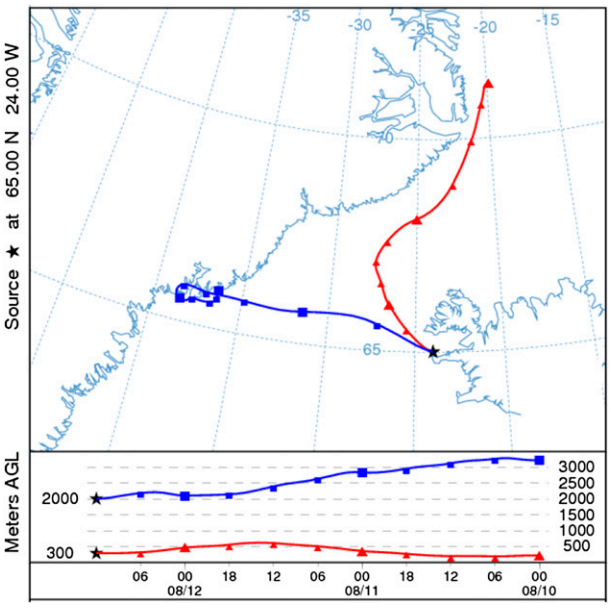

FIG. 6. Trajectories of air masses ending at 300 and 2000 m MSL at Mt. Snæfellsjökull at 1200 UTC 12 Aug 2009, calculated using the Hybrid Single-Particle Lagrangian Integrated Trajectory (HYSPLIT) provided online by NOAA.

as well as the February and July minima correspond to the variability of the frequency of northwesterly winds as well as variability in the mean static stability.

5. Discussion

A number of morphological and dynamical parameters of the flow and the vortices are given in Table 1. The

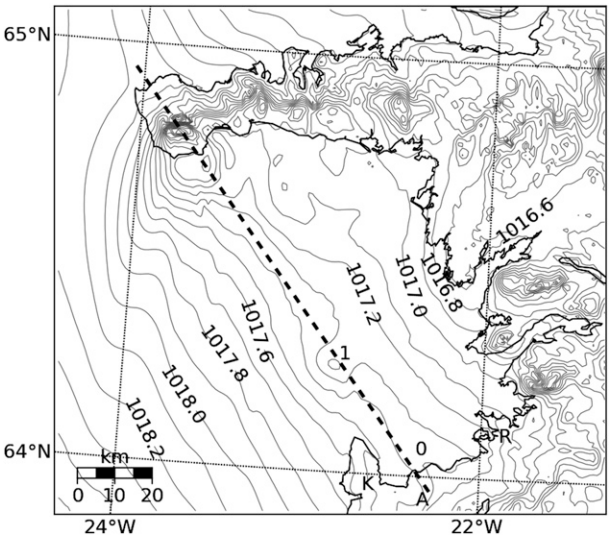

FIG. 7. Simulated surface pressure (hPa) at 1-km resolution at 1200 UTC 12 Aug 2009. Also marked are the locations of Reykjavík (R), vortices 0 and 1, as well as the cross section in Fig. 10 across Mt. Snæfellsjökull and Faxaflói bay (dashed line).

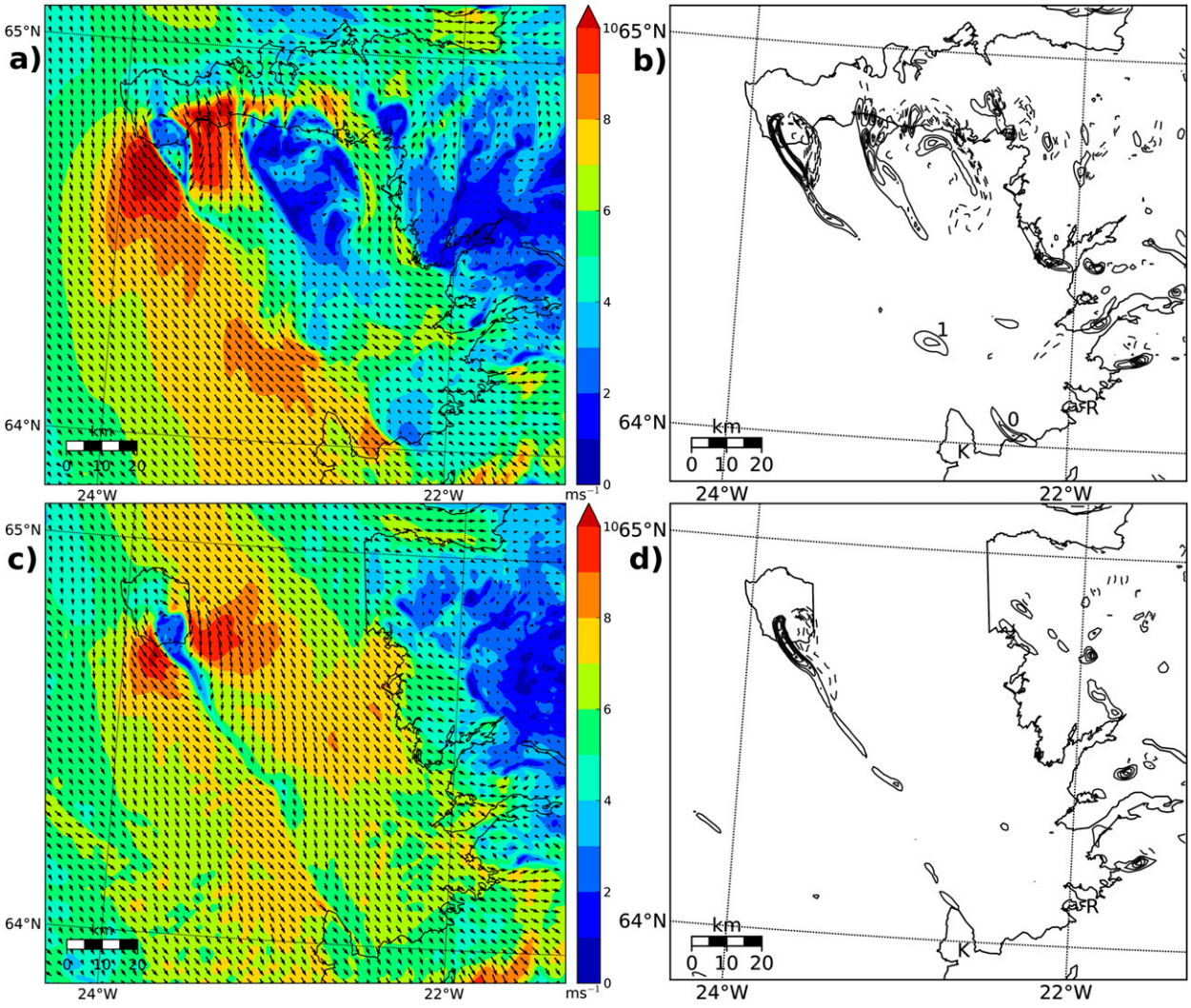

FIG. 8. Simulated winds (m s^{-1}) with intervals of 1 m s^{-1} and vertical vorticity (s^{-1}) with intervals of 100 s^{-1} at a model level close to 35 m above the ground (a),(b) with true topography and (c),(d) with no mountains in the Snæfellsnes peninsula east of Mt. Snæfellsjökull. Negative vorticity is indicated with dashed isolines. The zero isoline is omitted.

Brunt–Väisälä frequency N and the wind speed are calculated from the radiosounding by averaging through a layer below the mountain-top level [see aspects of flow blocking and calculations of N in vertically structured flow in Ólafsson (1996b), chapter 5, and the extensive numerical experiments of Reinecke and Durran (2008)]. The parameter a is the along-flow distance between vortices, and b is the across-flow distance between vortices [same as h in Heinze et al. (2012) and Young and Zawislak (2006)].

The critical height for wave breaking h_c is estimated from linear theory {using U and N as in Table 1 and estimating stagnation aloft [curve A in Smith's (1989a) flow diagram] for aspect ratio 1 to be close to $Nh/U = 1.2$} and numerical simulations by Ólafsson (1996a) and Ólafsson and Bougeault (1996). The Reynolds number (Re) is defined as $h/(\mathrm{CD} \times L)$ as in Smith et al. (1997), where h is mountain height, L is a length scale, and CD is the surface drag, set to 0.001 (Stull 1988, chapter 7). The Fr (div) is the Froude number based on the height of the dividing streamline (h_{div}) calculated using the equation $\mathrm{Fr(div)} = 1 - h_{\mathrm{div}}/H$, where H is the mountain height (e.g., Snyder et al. 1985; Etling 1989); h_{div} is determined from the simulated flow, defined as the upstream height of the lowest isentrope that reaches the mountain top.

The shallow-water Froude number [Fr (sw)] is calculated using Eq. (24) in Schär and Smith (1993a), the Strouhal number is defined as $L/(T_e U)$, and the Rossby number is $U/(fL)$, where f is the Coriolis parameter and T_e is the period of vortex shedding.

A key parameter for the classification of the flow is the nondimensional mountain height (Nh/U), often referred to as the inverse Froude number. According to Snyder

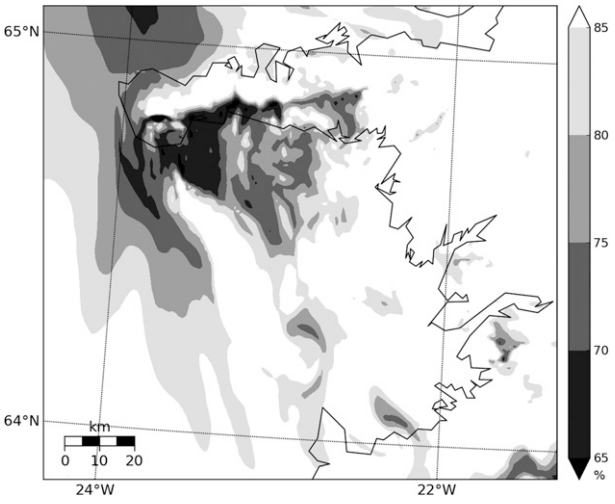

FIG. 9. Simulated maximum humidity (%) in the lowest 2000 m of the atmosphere.

et al. (1985) (see also Etling 1989, 1990), a Froude number (based on the above definition of N) below 0.4 is a prerequisite for vortex shedding. This limit should of course not be taken too literally for real flows with nonuniform vertical profiles, but according to Table 1, the present case is very close to this limit. However, in terms of the Froude number calculated from the height of the dividing streamline [Fr(div)] in Table 1, the present case is not close to the upper limit for vortex shedding. The difference between the values of the two Froude numbers presented in Table 1 lies in the vertical variability of the stability and the wind speed. The strongest winds are in a near-neutral layer well below mountain-top level, capped by the inversion with high N and weak winds. Consequently, the dividing streamline is almost as high as the mountain itself. A vertical redistribution of N and U giving lower N and greater U immediately below the mountain-top level would lead to a larger part of the flow being able to flow over the mountain and a Fr(div) closer to Fr.

In terms of the topographic data and the morphological and dynamic parameters in Table 1, the present case falls close to the laboratory and real cases studied by Etling (1990). However, In terms of morphology, our case is quite different from the classical Jan Mayen Island vortices, which are typically quasi symmetric with alternating direction of rotation. The present case does not have symmetric and counterrotating vortices [$b/d = 0$ and $a/b = \infty$, see Young and Zawislak (2006)]. Yet, Jan Mayen has a very similar h/L ratio. The Jan Mayen Froude number (which is based on the dividing streamline) is higher than in our case, but similar to the N-based Froude number in our case (U/Nh). Most Jan Mayen cases, such as the 6 June 2001 event (Heinze et al.

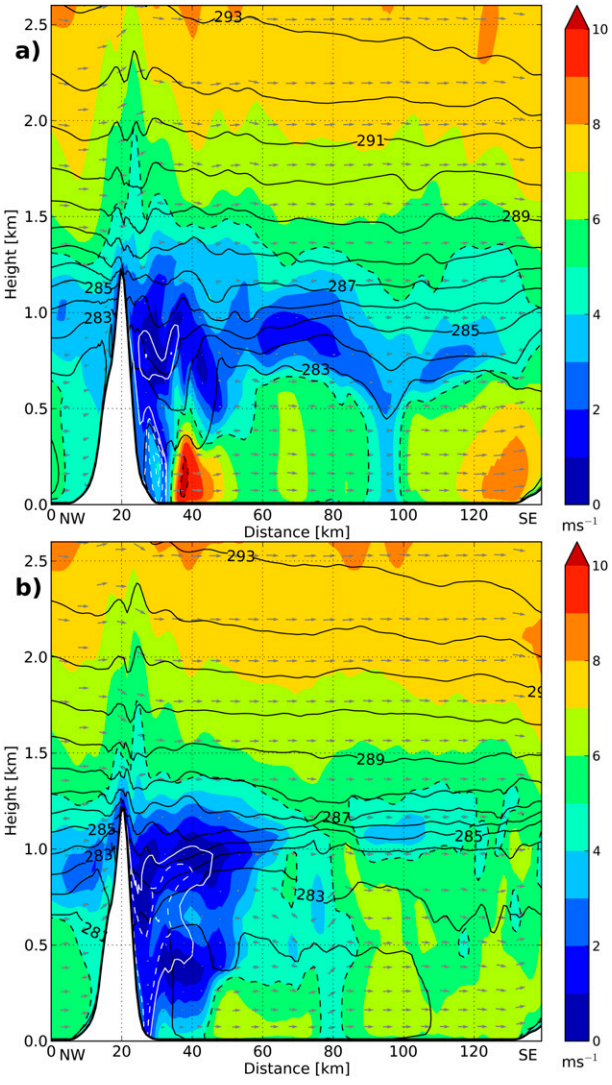

FIG. 10. (a) Wind speed (m s^{-1}), wind vectors, turbulence kinetic energy (J kg^{-1}), and isentropes (K) in section A across Faxaflói Bay, simulated at 1 km at 1200 UTC 12 Aug 2009. Also shown is orography, dashed line at 4 m s^{-1}, stagnant flow with a white line (0 m s^{-1}), and reversed flow with white dashed lines at 1 m s^{-1} intervals. (b) As in (a), but with no mountains on the Snæfellsnes peninsula, east of Mt. Snæfellsjökull.

2012) do, however, have a larger Rossby number due to stronger winds. There are, on the other hand, weak wind cases at Jan Mayen with a clear asymmetry in favor of the cyclonic vortices (e.g., 5 April 2012). Such an asymmetry is also evident in the experiments of Heinze et al. (2012, in their Fig. 11a). Mt. Snæfellsjökull is slightly steeper on the west side than on the east side. This contributes to a sharper shearline and more concentrated vorticity on the cyclonic (west) side of the wake (Fig. 8). This favors the cyclonic vortices. The removal of the mountains to the east of Mt. Snæfellsjökull results not only in stronger winds in their wake, but also upstream of the

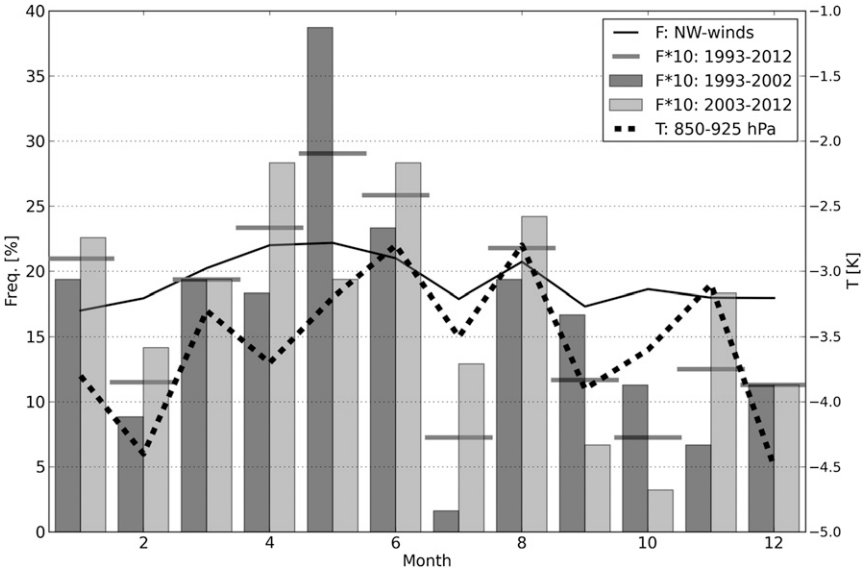

FIG. 11. Seasonal variability of the following parameters: frequency of winds from the northwest quadrant at 850 hPa (solid line), mean temperature difference between 850 and 925 hPa (T at 850 hPa minus T at 925 hPa: high value means strong mean static stability) in K (dotted line) and frequency of flow [% of time ($\times$10)] from the northwest quadrant at 850 hPa featuring an inversion between 925 and 850 hPa (columns and short solid horizontal lines). Based on radiosoundings at 0000 and 1200 UTC at Keflavik Airport (WMO 04018) 1993–2012.

entire peninsula and a slight drop in the height of the top of the boundary layer. As the upstream winds increase, the (N based) Froude number increases. This increase is only of the order of 0.1, but as the Froude number of 0.4 is close to the critical value for vortex shedding, it is not entirely surprising that there is only a wavy wake with no clear shedding vortices when the mountains are removed. This underlines not only the strong sensitivity of the vortices to the characteristics of the flow in which they are embedded, but it suggests that the Froude number based on a simple averaging of U and N separately, below mountain-top level, is indeed predictive for the downstream flow as it is in idealized flow configurations.

The present case falls far into regime III in Schär and Smith (1993a, their Fig. 3) with high h/Z_i (''M'' in Schär and Smith 1993a) and a low shallow-water Froude number. Regime III has a pierced fluid surface and a wake with a reversed flow. As in Schär and Smith (1993a), the simulated flow shows a pattern of hydraulic jump or small-scale gravity wave breaking close to the mountain. Downstream, there is a circular region of low pressure (Fig. 7) and a dip in the isentropes at the top of the boundary layer (Fig. 11) corresponding to a local lowering in the height of the fluid associated with the vortices in Schär and Smith (1993b).

To the extent that the regime thresholds are known, the parameters in Table 1 place the current case well within the regime of a wake with eddy shedding defined by the work of Schär and Smith (1993a,b) and Grubišić et al. (1995) as presented in Fig. 1 in Smith et al. (1997). Unlike the ''weak wake'' flow in Smith et al. (1997), our case features clear vortices that are advected downstream. The height of the mountain is far above the threshold of breaking waves and the fact that the inversion is well below mountain-top level provides a clear upstream blocking of most of the flow below mountain-top level. The low surface friction and small horizontal scale provide a sufficiently high Reynolds number for shedding of the vortices.

The qualitative structure of the vortices is reproduced in the numerical simulation and elements such as a warm core and cloud pattern are comparable with the vortices simulated and Heinze et al. (2012). In fact, the commalike cloud structure resembles very much a typical Jan Mayen vortex street (e.g., Heinze et al. 2012, their Fig. 1), apart from the absence of the counter-rotating vortices.

Finally, the Strouhal number of our case is calculated to be 0.3, which is within the range of vortex shedding (Atkinson 1981, referenced by Schär and Smith 1993b), but close to the upper limit of the shedding range.

The seasonal variability calls for some discussion. The static stability cycle reflects the cooling of the air by the ocean surface in the summer and the warming of the air by the ocean surface in the winter. The result that the

TABLE 1. Fundamental morphological and dynamical parameters of the flow: N is the Brunt–Väisälä frequency; U is the wind speed; h is mountain height; L is a characteristic length scale and the diameter of the mountain; a is the along-stream distance between vortices; CD is surface drag; Z_i is the height of the inversion; T_e is the period of vortex shedding; h_c is a critical mountain height for internal wave breaking; b is the cross-flow distance between vortices; Fr is the Froude number and Fr (div) and Fr (sw) are the Froude numbers based on the dividing streamline and shallow water, respectively; St is the Strouhal number; Ro is the Rossby number; and Re is the Reynolds number.

N	U	h	L	a	CD	Z_i	T_e	h_c	h/Z_i	h/d	a/h	h/L	h/h_c	Nh/U (Fr)	Fr (div)	Fr (sw)	St	Ro	Re
$0.009\,s^{-1}$	$5\,m\,s^{-1}$	1400 m	10 km	30 km	0.001	1000 m	2 h	600 m	1.4	0	∞	0.14	2.3	2.5 (0.4)	0.05	0.2	0.3	4	100

northwesterly flow is more frequent in late winter than in the autumn is in line with frequency of blockings to the southwest of Iceland (Barriopedro et al. 2006, from their Fig. 7). In fact, favorable conditions for wake flow as defined in Fig. 11 are almost exclusively when there is a stationary high to the southwest of Iceland (see Fig. 12). The February minimum coincides with high frequency of southerly winds (Ólafsson and Ágústsson 2007; Jónsson 2002) as the storm track is anomalously meridional and lies between Iceland and Greenland. The July minimum coincides with the time of the year when thermally driven mesoscale flow is frequent. Heating of the low-level air leads to a high at 850 hPa over Iceland (close to the top of the boundary layer), generating southerly flow over the Faxaflói Bay. The relatively high frequency of wake flow in January is neither reflected in the mean of the northwesterly winds nor in the mean static stability, which is low in January. This underlines the fact that the frequency or likelihood of events may not be reflected in the mean values of individual flow features of which they are composed.

The implications of the present study on local weather forecasting needs to be highlighted. First, we have confirmed that vortices in the clouds at the top of the boundary layer are connected with circulation at the surface (Fig. 4). Nowcasts of wind direction may therefore benefit from detection and consideration of cloud patterns like those described in this paper. Second, forecasts up to far downstream of Mt. Snæfellsjökull in weak winds with low-level inversions may not be very reliable in terms of the persistence of wind direction. That may be important for not only the distribution of pollutants (certain management of waste may only take place in favorable and persistent winds), but also for temperature and concentration of pollen. In weak wind situations, there can be very strong gradients in these parameters along the coast. Correct forecast of wind direction and probability of a change in the wind direction is therefore very important for local forecasts of temperature and pollen. Finally, the fact that only one of the PBL schemes reproduced the vortices underlines how sensitive these flow features can be to subgrid processes.

6. Summary and conclusions

In this paper, a series of satellite images, an atmospheric sounding, surface-based weather observations, as well as high-resolution atmospheric simulations have been used to explore an interesting case of vortices traveling in the atmospheric boundary layer. The vortices were asymmetrically shed from Mt. Snæfellsjökull on the Snæfellsnes peninsula in West Iceland and advected 120 km across the ocean until they made landfall in Reykjavík where the progress of one of the vortices farther inland was documented by surface-based observations. The flow is characterized by high-nondimensional mountain height (low Froude number) and a Rossby number indicating nonnegligible effects from the Coriolis force. In general, the parameters governing the flow do predict an upstream blocking and a wake with vortex shedding according to previous results on stratified and shallow-water flows. The flow resembles in all main aspects flows that lead to typical Jan Mayen vortex streets, except that in this case, the Rossby number is somewhat lower, there are hardly any winds at mountain-top level, and Mt. Snæfellsjökull is not quite symmetric in the sense that a low mountain range blocks some of the

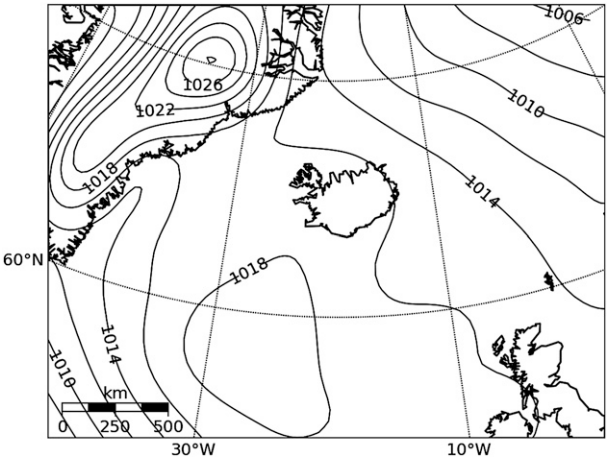

FIG. 12. A composite mean sea level pressure (hPa) in cases of Mt. Snæfellsjökull wake flow in January 1993–2012 as defined in Fig. 11. Based on data from NOAA.

low-level flow on its east side and that the west side of Mt. Snæfellsjökull is steeper than its east side. The asymmetry of the shape of Mt. Snæfellsjökull and geostrophic adjustment are most likely responsible for the fact that the vortices in the present case do not form a symmetric pattern of counter-rotating vortices, like in a typical Jan Mayen vortex street case. Geostrophic adjustment with a Rossby number of 4 or even less at the inversion level also appears to play a role. Needless to say, it is very hard to forecast winds and cloudiness inside a mountain wake with shedding vortices, even only a few hours ahead. Not only is the timing of the passing of the vortices uncertain, but so is the exact location of landfall.

Acknowledgments. This study has been partly funded by the Icelandic Research Fund (RANNÍS). The authors are grateful for comments from three anonymous reviewers.

REFERENCES

Ágústsson, H., and H. Ólafsson, 2012: The bimodal downslope windstorms at Kvísker. *Meteor. Atmos. Phys.,* **116,** 27–42, doi:10.1007/s00703-010-0075-y.

Atkinson, B. W., 1981: *Meso-Scale Atmospheric Circulations*. Academic Press, 495 pp.

Barriopedro, D., R. Garcia-Herrera, A. R. Lupo, and E. Hernandez, 2006: A climatology of Northern Hemisphere blocking. *J. Climate,* **19,** 1042–1063, doi:10.1175/JCLI3678.1.

Etling, D., 1989: On atmospheric vortex streets in the wake of large islands. *Meteor. Atmos. Phys.,* **41,** 157–164, doi:10.1007/BF01043134.

——, 1990: Mesoscale vortex shedding from large islands: A comparison with laboratory experiments of rotating stratified flows. *Meteor. Atmos. Phys.,* **43,** 145–151, doi:10.1007/BF01028117.

Grubišić, V., R. B. Smith, and C. Schär, 1995: The effect of bottom friction on shallow-water flow past an isolated obstacle. *J. Atmos. Sci.,* **52,** 1985–2005, doi:10.1175/1520-0469(1995)052<1985:TEOBFO>2.0.CO;2.

Heinze, R., S. Raasch, and D. Etling, 2012: The structure of Kármán vortex streets in the atmospheric boundary layer derived from large eddy simulation. *Meteor. Z.,* **21,** 221–237, doi:10.1127/0941-2948/2012/0313.

Hong, S.-Y., Y. Noh, and J. Dudhia, 2006: A new vertical diffusion package with an explicit treatment of entrainment processes. *Mon. Wea. Rev.,* **134,** 2318–2341, doi:10.1175/MWR3199.1.

Hunt, J. C. R., Y. Feng, P. F. Linden, M. D. Greenslade, and S. D. Mobbs, 1997: Low Froude number flows past mountains. *Nuovo Cimento,* **20,** 261–272.

Jónsson, T., 2002: Sveiflur III. Árstíðasveiflur á Íslandi. Veðurstofa Íslands, Reykjavík, Iceland. Tech. Rep. 02033, 21 pp. [Available online at http://www.vedur.is/utgafa/greinargerdir/2002.]

Ólafsson, H., 1996a: Atlas des écoulements hydrostatiques autour d'un relief idealisé. Tech. Rep. 42, CNRM, Météo France, Toulouse, France, 86 pp. [Available online at http://www.vedur.is/media/vedurstofan/utgafa/greinargerdir/1995/Groupe_de_meteorologie_20120904_1.pdf.]

——, 1996b: Morphologie et traînée de quelques écoulements orographiques de complexité croissante. Ph.D. dissertation, Université Paul Sabatier, France, 313 pp.

——, and P. Bougeault, 1996: Nonlinear flow past an elliptic mountain ridge. *J. Atmos. Sci.,* **53,** 2465–2489, doi:10.1175/1520-0469(1996)053<2465:NFPAEM>2.0.CO;2.

——, and H. Ágústsson, 2007: The Freysnes downslope windstorm. *Meteor. Z.,* **16,** 123–130, doi:10.1127/0941-2948/2007/0180.

Reinecke, P. A., and D. R. Durran, 2008: Estimating topographic blocking using a Froude number when the static stability is nonuniform. *J. Atmos. Sci.,* **65,** 1035–1048, doi:10.1175/2007JAS2100.1.

Schär, C., and R. B. Smith, 1993a: Shallow-water flow past isolated topography. Part I: Vorticity production and wake formation. *J. Atmos. Sci.,* **50,** 1373–1400, doi:10.1175/1520-0469(1993)050<1373:SWFPIT>2.0.CO;2.

——, and ——, 1993b: Shallow-water flow past isolated topography. Part II: Transition to vortex shedding. *J. Atmos. Sci.,* **50,** 1401–1412, doi:10.1175/1520-0469(1993)050<1401:SWFPIT>2.0.CO;2.

——, and D. R. Durran, 1997: Vortex formation and vortex shedding in continuously stratified flows past isolated topography. *J. Atmos. Sci.,* **54,** 534–554, doi:10.1175/1520-0469(1997)054<0534:VFAVSI>2.0.CO;2.

Shin, H. H., and S.-Y. Hong, 2011: Intercomparison of planetary-boundary layer parameterizations in the WRF model for a single day from CASES-99. *Bound.-Layer Meteor.,* **139,** 261–281, doi:10.1007/s10546-010-9583-z.

Skamarock, W. C., J. B. Klemp, J. Dudhia, D. O. Gill, D. M. Barker, W. Wang, and J. G. Powers, 2005: A description of the advanced research WRF version 2. Tech. Rep. NCAR/TN-468+STR, 88 pp. [Available online at http://www.mmm.ucar.edu/wrf/users/docs/arw_v2.pdf.]

Smith, R. B., 1989a: Hydrostatic air-flow over mountains. *Advances in Geophysics,* Vol. 31, Academic Press, 1–41.

——, 1989b: Comment on ''Low Froude number flow past three-dimensional obstacles. Part I: Baroclinically generated lee vortices.'' *J. Atmos. Sci.,* **46,** 3611–3613, doi:10.1175/1520-0469(1989)046<3611:COFNFP>2.0.CO;2.

——, A. C. Gleason, P. A. Gluhosky, and V. Grubišić, 1997: The wake of St. Vincent. *J. Atmos. Sci.,* **54,** 606–623, doi:10.1175/1520-0469(1997)054<0606:TWOSV>2.0.CO;2.

Smolarkiewicz, P. K., and R. Rotunno, 1989a: Low Froude number flow past three dimensional obstacles. Part I: Baroclinically generated lee vortices. *J. Atmos. Sci.,* **46,** 1154–1164, doi:10.1175/1520-0469(1989)046<1154:LFNFPT>2.0.CO;2.

——, and ——, 1989b: Reply. *J. Atmos. Sci.,* **46,** 3614–3617, doi:10.1175/1520-0469(1989)046<3614:R>2.0.CO;2.

Snyder, W. H., R. S. Thomson, R. E. Eskridge, R. Lawson, I. P. Castro, S. T. Lee, J. C. R. Hunt, and J. Ogawa, 1985: The structure of strongly stratified flows over hills: Dividing streamline concept. *J. Fluid Mech.,* **152,** 249–228, doi:10.1017/S0022112085000684.

Stull, R. B., 1988: *An Introduction to Boundary-Layer Meteorology*. Kluwer Academic Publishers, 666 pp.

Young, G. S., and J. Zawislak, 2006: An observational study of vortex spacing in island wake vortex streets. *Mon. Wea. Rev.,* **134,** 2285–2294, doi:10.1175/MWR3186.1.